


Review

Applications of High-Pressure Technology for High-Entropy Alloys: A Review

Wanqing Dong ¹, Zheng Zhou ¹, Mengdi Zhang ¹, Yimo Ma ¹, Pengfei Yu ^{1,*}, Peter K. Liaw ² 
and Gong Li ^{1,*}

¹ State Key Laboratory of Metastable Materials Science and Technology, Yanshan University, Qinhuangdao 066004, China

² Department of Materials Science and Engineering, The University of Tennessee, Knoxville, TN 37996-2200, USA

* Correspondence: ypf@ysu.edu.cn (P.Y.); gongli@ysu.edu.cn (G.L.)

Received: 23 June 2019; Accepted: 26 July 2019; Published: 8 August 2019



Abstract: High-entropy alloys are a new type of material developed in recent years. It breaks the traditional alloy-design conventions and has many excellent properties. High-pressure treatment is an effective means to change the structures and properties of metal materials. The pressure can effectively vary the distance and interaction between molecules or atoms, so as to change the bonding mode, and form high-pressure phases. These new material states often have different structures and characteristics, compared to untreated metal materials. At present, high-pressure technology is an effective method to prepare alloys with unique properties, and there are many techniques that can achieve high pressures. The most commonly used methods include high-pressure torsion, large cavity presses and diamond-anvil-cell presses. The materials show many unique properties under high pressures which do not exist under normal conditions, providing a new approach for the in-depth study of materials. In this paper, high-pressure (HP) technologies applied to high-entropy alloys (HEAs) are reviewed, and some possible ways to develop good properties of HEAs using HP as fabrication are introduced. Moreover, the studies of HEAs under high pressures are summarized, in order to deepen the basic understanding of HEAs under high pressures, which provides the theoretical basis for the application of high-entropy alloys.

Keywords: high-entropy; high pressure; high pressure torsion; diamond anvil cells

1. Introduction

Emerging in recent years, high-entropy alloys (HEAs) are newly developed alloys, with many outstanding properties which have broken the design concept of traditional alloys, and have a variety of principal elements and special crystal structures. Although the composition of the high-entropy alloys varies, the phase composition is very simple. Usually only one or two solid-solution phases are detected by X-ray diffraction, and rare intermetallic compounds are formed. Since there is no principal element in HEAs, the performance of the alloy is affected by the combined influence of the constituent elements. As a result, the performance of HEAs is somewhat unpredictable. The structure and stability of the alloy has crucial influence on its properties. Therefore, it is necessary to study the structures, and the stability of the structure of the different HEAs under various conditions. HEAs are solid solutions composed of many elements which can maintain their stable structures under normal temperatures and atmospheric pressure. However, during long-term or high-temperature annealing, the new phase will be created, which will affect the performance of the alloy [1–3]. The pressure, temperature, and chemical composition are the basic thermodynamic factors that determine the state of a substance. The use and control of temperature and chemical composition are almost synchronous

with the development of human civilization. However, due to the limitations of technical conditions, the application of pressure has just begun. High-pressure technology is a relatively-young and emerging discipline, but most of the condensed matter in the universe is under high pressure. The research on high pressures relies heavily on the experimental techniques, and each progression of the method has led to a significant expansion of our basic understanding of material behavior under high pressures. The progress in high-pressure experimental technology has directly promoted the development of the high-pressure science and provided an advanced method for frontier subjects. It has become an important field in modern scientific research. There are few studies on the structures of HEAs under high pressures. Interactions within the materials will change under high pressures and induce the generation of high-pressure phase transitions, thus becoming a new material with special properties. The materials will show many unique properties under high pressures, ones which do not exist under normal conditions, providing a subject for the in-depth study of materials. The behavior of HEAs under high pressures is a potential research direction for the future.

2. High-Entropy Alloys (HEAs)

2.1. Concept

HEAs are kinds of alloys developed in recent years. HEAs are loosely defined as solid-solution alloys that contain more than five principal elements in an equal or near-equal atomic percent (at. %) [4]. These kinds of alloys were defined by Yeh et al. [4] in 2004 as HEAs, and in the same year named by Cantor [5] et al. as the multi-component alloy. The concept of HEAs is based on the development of bulk amorphous alloys in the 1990s, when people were looking for alloys with ultra-high glass-forming ability. According to the well-known confusion principle, the more components of the alloy, the higher the chaos of the liquid alloy. That is, with a high entropy of mixing, it is easy for the alloy to retain the structure of the melt, thus forming a disordered amorphous structure. Figure 1 shows a panoramic view of the materials that humans have used over the past 10,000 years. The picture gives different types of materials, from ceramics to metals, polymers, and most recently composites, the same age at which HEA production is noted. With an increasing understanding of HEAs, the requirements for the content of each element and the number of elements have gradually loosened in the definition of HEA. At present, quaternary equiatomic or part of non-equiatomic quaternary alloys are also defined as HEAs [6–8], and some literature now refers to multi-component alloys containing small amounts of intermetallic compounds as HEAs [9,10].

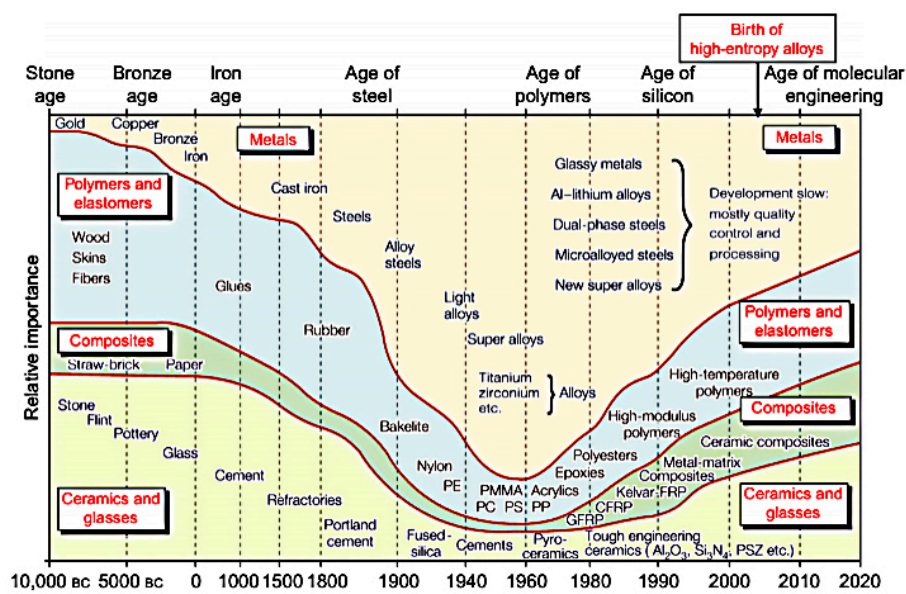


Figure 1. Historical evolution of engineering materials [11].

2.2. Four Core Effects

Yeh [12] summarized the four core effects in HEAs. Those were: (1) High-entropy effects; (2) sluggish diffusion; (3) severe lattice distortion; and (4) cocktail effects.

2.2.1. High-Entropy Effects

This is the most important characteristic of the HEA; i.e., the formation of intermetallic compounds or complex phases is inhibited due to the high entropy of the HEAs, tending to form solid-solution phases [4,5,13,14]. In other words, the high entropy produced by multiple principal elements can inhibit the generation of intermetallic compounds.

2.2.2. Sluggish Diffusion

In traditional alloys, there is a high probability that a less prevalent atom is surrounded by the main element's atoms, which are called the solute atoms. It means that during the atom diffusion, the interaction with the surrounding atoms is essentially constant. However, the atoms that surround an atom in the HEAs are diverse, leading to different activation energies required by various lattice sites during atomic diffusion in HEAs [15]. In comparison with traditional alloys, more energy is needed during the atomic diffusion for HEAs. Although diffusion activation varies greatly with the elements, the trend of the increased diffusion activation energy can be obtained from low entropy to high entropy.

The sluggish diffusion theoretically suppresses the grain growth in HEAs [4] and explains the formation of nano-sized precipitates. On the other hand, the sluggish diffusion increases the phase stability of HEAs, especially at high temperatures; the phase stability and high-temperature strength even exceed some Ni-based superalloys [16].

2.2.3. Severe Lattice Distortion

In HEAs, each atom is surrounded by other kinds of atoms. Due to different compositional atomic sizes in HEAs, that feature can lead to the severe lattice distortion. The severe lattice distortion affects the mechanical, physical, and chemical properties of the material. As shown in Figure 2, the probability that each element in the HEA occupies the position of the lattice is the same, and the atomic radii of different atoms will cause severe lattice distortion.

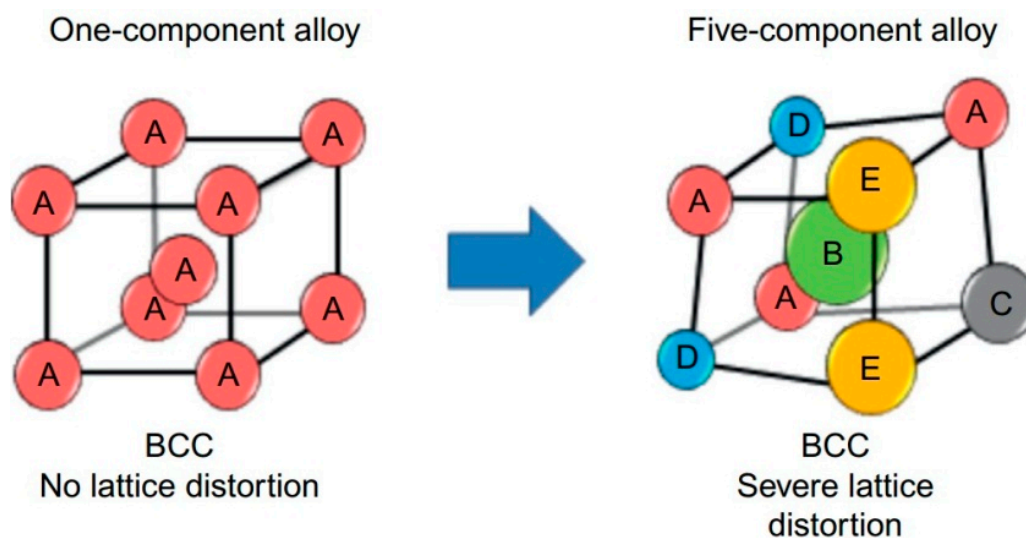


Figure 2. Schematic illustration of lattice distortion.

2.2.4. Cocktail Effect

The cocktail effect for alloys was first mentioned by Ranganathan [17] to describe some basic characteristics of the elements affecting the properties of alloys. However, for the HEAs that break through the traditional design concept, the cocktail effect does not mean that the performance of the alloys is simply a superposition of the properties of each component. There are also interactions between different elements that eventually lead to a composite effect in HEAs [12].

2.3. Research Status

Due to the four core effects of HEAs, many HEAs exhibit mechanical, physical, and chemical properties that are superior to pure metals and other alloys. Many research groups have carried out much research on HEAs. At present, several mature high-entropy systems have been formed, including $Al_xCoCrCuFeNi$ [4], $CoCrFeMnNi$ [5], $WNbMoTaV$ [8], and $GdTbDyTmLu$ [18]. The structures and properties can be regulated through a series of elemental additions or changes in the content, such as the addition of Ti [19], Zr [20], B [20], V [21], and/or Mo [22,23]. Some HEAs have the high glass-forming ability, such as $PdPtCuNiP$ [24], $ScCaYbMgZn$ [25], and $ZrHfTiCuFe$ [26]. The structures of the HEAs include all the three simple metal crystal structures: A face-centered-cubic (fcc) structure represented by $CoCrFeNi$, a body-centered-cubic (bcc) structure represented by $TaZrHfNbTi$, and a hexagonal-closed-packed (hcp) structure represented by $YGdTbDyLu$. The deformation mechanisms of hcp-phase metals have been summarized: Either tensile or compressive strain induced twins or basal and prismatic slips [27–29].

In addition to the excellent mechanical properties of the HEAs at room temperature, the HEAs also have good performance under extreme conditions, such as high and low temperatures. The $VNbMoTaW$ alloy developed by Senkov et al. maintains a yield strength of 800 MPa at 600 to 800 °C, and the yield strength is still more than 400 MPa at 1600 °C [30]. The $CoCrFeMnNi$ single-phase fcc alloy demonstrates the characteristics of “lower temperature and more toughness,” and the fracture toughness value is greater than 200 $MPa \cdot m^{1/2}$ at a low temperature (77 K) [31]. For $Co_{1.5}CrFeNi_{1.5}Ti$ and $Al_{0.2}Co_{1.5}CrFeNi_{1.5}Ti$ HEAs, the wear resistance is at least twice that of conventional wear-resistance steels, such as SUJ and SKH51 steel under similar hardness conditions [32]. Moreover, the mechanism of the phase transition in HEAs has received great attention from researchers. At present, the transformation-induced plastic deformation and polymorphism have been studied [7,33]. However, the phase-transition kinetics of the HEAs still need to be further studied. The atomic mechanism and thermodynamic principle of the HEA phase transition are still in dispute [34,35]. Surface energy at the interface may affect the solidification and diffusion of solids, such as precipitation, resulting in phase transitions [36].

3. High Pressure

The rapid development of the high-pressure technology and the interpenetration with other technologies have become a hot topic in science today. High pressure is an important means to control the properties of the material, and is a decisive variable in modern scientific research [37]. Bundy synthesized diamond with technologies employing high pressures and high temperatures, which paved the way for the high-pressure technology for the application of new materials [38].

According to the different high-pressure loading methods or technologies, the high-pressure experimental technology can be divided into the static high-pressure loading technology and dynamic high-pressure loading technology. The duration of the traditional, dynamic high-pressure experiments is very short, typically no more than a few milliseconds, and can reach very high pressures and temperatures. However, the defects are also obvious: The time span is too short to be effectively detected and accurately controlled, and the large amount of extra heat will affect the expected experimental results. In contrast, the static high-pressure technique can perform the non-destructive research on the material under fixed pressure conditions and can obtain good data. Static and dynamic high pressures are complementary to each other, which enhances our basic understanding of the

material structure and performance under different high pressures. The dynamic high-pressure loading technology is an experimental technique for subjecting samples to transient high-pressure and high-temperature environments by the shock waves or high-speed physical impact generated from an explosion, or other means. At present, there are many experimental techniques that can achieve dynamic high pressures, which can be simply divided into high-speed dynamic loading and low-speed dynamic loading. The methods implementing the former mainly include the underground nuclear explosion, magnetic flux compression, rapid expansion, or an explosion of air currents. These methods are characterized by fast loading (can realize nanosecond loading), and high-pressure limits. But it is difficult to accurately control the pressure range, relying heavily on experience and repeated experiments. Many high-speed dynamic-loading methods are still in development and inappropriate for research under normal laboratory conditions. In contrast, the experimental techniques of low-speed dynamic loading are relatively mature and have mostly been used in experiments. These loading techniques have a large time span (from hours to milliseconds or even microseconds), high repeatability, high-pressure loading accuracy, and wide adaptation (which can be applied to room temperature, high temperature, low temperature, magnetic field, and other conditions), which can be combined with other test methods and characteristics. It is of great help to study the structures and properties of materials under nonequilibrium thermodynamic conditions, which is an important direction in the high-pressure research.

The static high-pressure loading method is a technique for obtaining high-pressure experimental conditions using a static compression method. The sample is slowly compressed by means of the external mechanical loading device. Since the compression process is slow enough, the heat generated in the process can be fully exchanged with the external environment. Hence, the static high-pressure loading process is an isothermal compression process. At present, the equipment to achieve the static high pressure mainly includes large cavity presses and diamond-anvil-cell presses. Currently, the highest pressure of the former is up to hundreds of thousands GPa, which is the main equipment for the synthesis of high-pressure materials, and it has a unique advantage in the use of high-temperature and high-pressure, synthetic block, superhard materials. Compared to the former, the diamond-anvil cell (DAC) is small in size, requires few samples, and has low experimental costs. Multiple in-situ experiments (including X-ray diffraction, Raman spectrum, etc.) can be performed under a variety of experimental conditions, and higher-pressure limits can be achieved. The hexahedron-anvil-press instrument is the most widely-used static high-pressure device. Figure 3 is the schematic of the instrument. The instrument is composed of six anvil cells, extruding a square-pressure transmitting medium, and the sample is wrapped in the medium. As shown in the figure, the machine applies the pressure from six directions to the center simultaneously to achieve the static equilibrium [39,40].

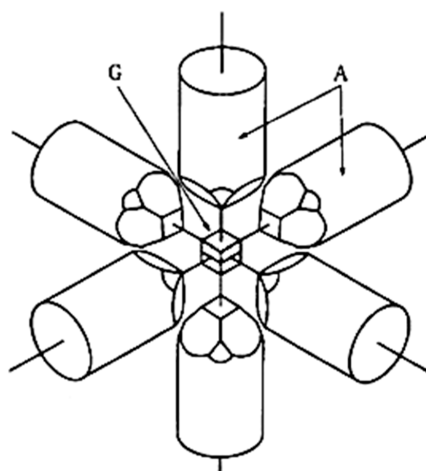


Figure 3. Schematic of the hexahedron anvil press.

The DAC, another device that can achieve the static high-pressure loading, it is smaller in size, and Figure 4 shows the principle of the DAC. DACs are composed of two opposing diamond anvils that squeeze the samples between them to create hydrostatic/non-hydrostatic pressures [41]. In 1977, Bruas combined the DAC technology with synchrotron-radiation X-ray diffraction for the first time [42], which greatly promoted the development of the high-pressure science. In 2015, Dubrovinsky et al. used nano-diamonds in combination with a two-stage pressurized device to obtain a high static pressure of 770 GPa [43]. The core of the DAC is to use the extremely-high hardness of the diamond, with two diamonds pressing on top of each other, to generate high pressures.

The high-pressure torsion (HPT) process was first proposed by Bridgman in 1935 [44]. With the development of microscopy technology, it was not until the 1980s that researchers discovered that ultra-fine crystalline structure could be prepared by high-pressure torsion technology [45]. The principle of HPT is exhibited in Figure 5. The sample is placed between the two anvils and subjected to extremely high pressures of hundreds of GPa. When there is a relative rotation between the two anvils driven by external forces, the friction between the sample and the anvils drives the sample to rotate and causes the shear deformation of the sample. Although the sample is subjected to the large strain plastic deformation, it will not rupture, due to the high pressure. By means of HPT, the size of crystal grains can be significantly reduced, and a dense nano-bulk material can be prepared effectively.

In high-pressure scientific research, the structure-phase transitions, which combine pressure or temperature and pressure as driving forces, can be divided into two basic types, namely reconstructive phase transitions and displacive phase transitions. The classification is based on whether the chemical bonds that form the periodic grid are destroyed after the phase transformation. In the process of the reconstructive phase transition, the main chemical bonds are broken and recombined to form a new structure. There is no clear orientation relationship with the previous phase in crystallography. All the reconstructive phase transitions belong to the first-order phase transition, and the discontinuity of the volume change during the phase transition is obvious. Since there are dynamic barriers between the equilibrium pressures of the adjacent two phases, it often leads to a hysteresis effect in the phase transition. The phase-transition pressure point in the pressurization process is greater than the pressure-relief process. The secondary bonds may break when a displacive phase transition occurs, but the main chemical bonds will not break, usually due to the displacement of the atoms or the tilt of the polyhedral structure. Under a high pressure, many phase transitions are displacive phase transitions, and the degree of the discontinuous volume change is very small. Most of them still belong to the first-order phase transition.

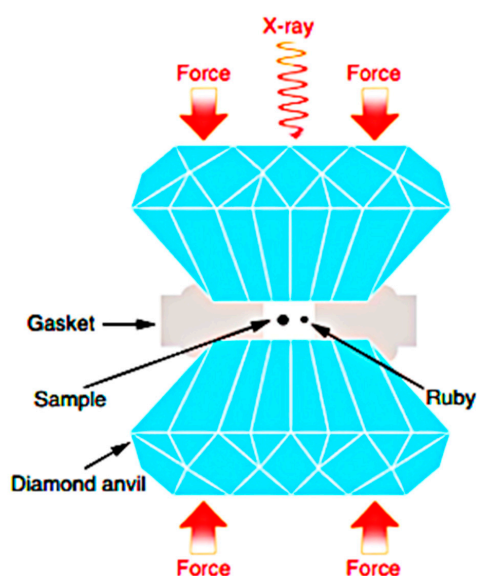


Figure 4. Schematic of the diamond anvil cell (DAC).

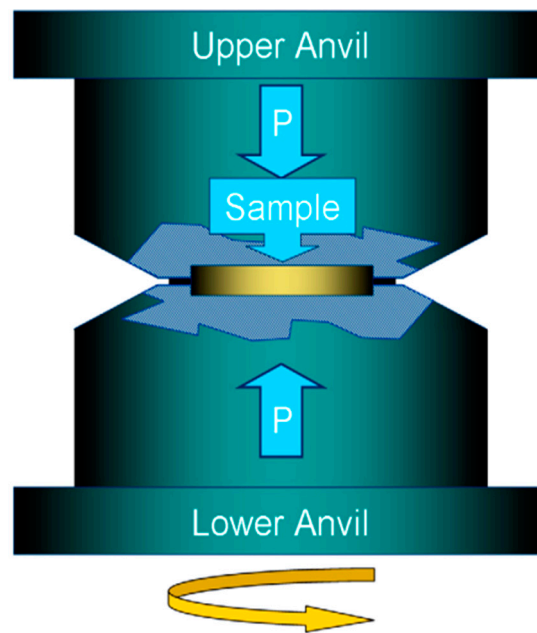


Figure 5. Schematic illustration showing the principles of high-pressure torsion (HPT).

4. HEAs under High Pressure

4.1. Dynamic High Pressure

The HEA is a new kind of alloy between the traditional alloy and the amorphous alloy. The deformation mechanism shows different characteristics from the traditional alloys. Therefore, it is necessary to study the structure and phase-transition process of HEAs under high pressures. The microstructures of HEAs under high pressures is also one of the hot topics in the alloy research. Huang et al. [46] developed a facile, two-step carbothermal shock (CTS) method that employs flash heating and cooling (temperature of 2000 K, shock duration of 55 ms, and ramp rates in the order of 10^5 K/s) of metal precursors on oxygenated-carbon support to produce HEA nanoparticles (HEA-NPs) with up to eight metallic elements. Figure 6 shows the scanning transmission electron microscopy (STEM) elemental maps for PtPdRhRuCe HEA-NPs. The aforementioned is a method of synthesizing HEAs using the high pressure produced by the thermal shock. Nanoparticles are useful in a wide range of applications. Huang et al. [46] developed a method for making HEA nanoparticles, and the “carbothermal shock synthesis” can be tuned to select for the nanoparticle size as well as final structure. These carbothermal shock (CTS) capabilities facilitate a new research area for the materials discovery and optimization.

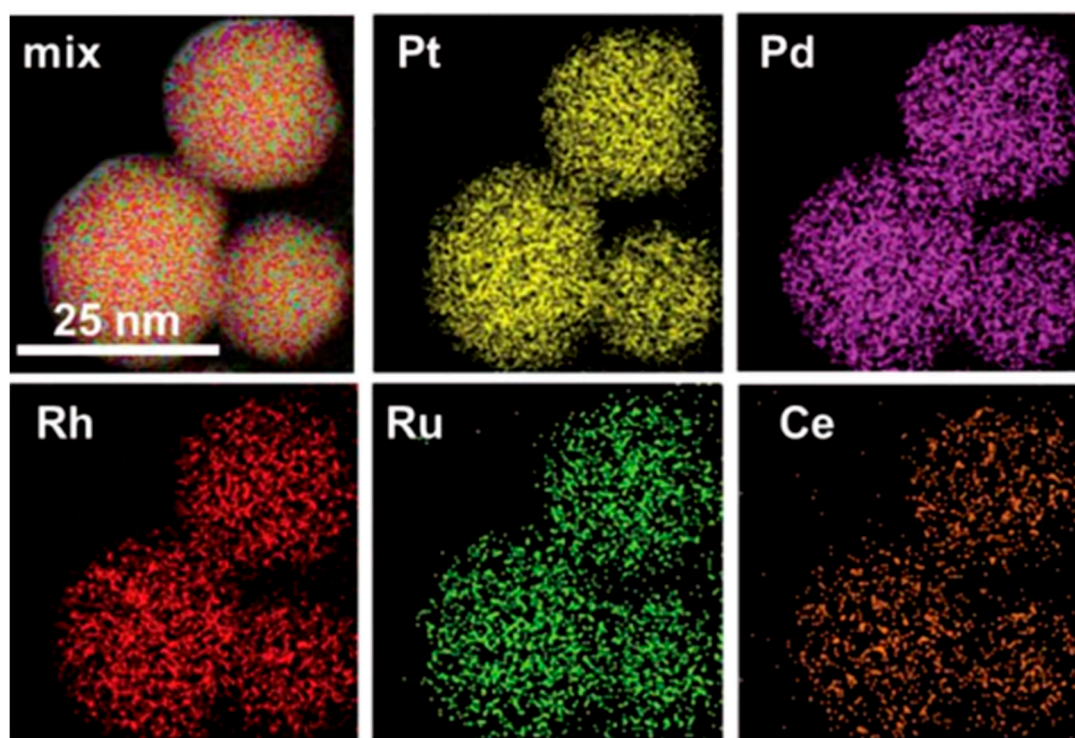


Figure 6. Scanning transmission electron microscope (STEM) elemental maps for PtPdRhRuCe high-entropy-alloy nanoparticles (HEA-NPs), reproduced from [46], with permission from authors.

4.2. Diamond Anvil Cells

The duration of traditional dynamic high-pressure experiments is very short, generally no more than a few milliseconds. Therefore, it is difficult to effectively detect and accurately control, and the large amount of the extra heat will affect the expected experimental results. Thus, the experiment of placing HEAs under high pressures usually adopts a static high-pressure technology. Yu et al. [47] used DAC to pressurize the rare-earth HoDyYGdTb HEA and studied the phase transition under high pressures. Figure 7 shows the pressure-volume relationship of different phases of the HoDyYGdTb HEA measured at room temperature, and the red line indicates the fitting result using the Birch-Murnaghan equation of the state in [48]. The sample was prepared by arc-melting, then scraped, and loaded into the T301-stainless-steel gasket hole with a diameter of 180 μm . The specimen was pressurized up to 60.1 GPa. The HEA is shown to follow the trivalent rare-earth crystal structure sequence of hcp \rightarrow Sm-type \rightarrow dhcp \rightarrow dfcc, which correlated the $s \rightarrow d$ charge transfer of the HEA. The bulk modulus and atomic volume of the rare-earth HEA agree extremely well with the calculated values with the “additivity law.” The pressure-included phase transformation among bcc, fcc, and hcp phases in transition metals were reported previously. What is most noteworthy is that Au changes the structure of HCP under extreme conditions [49]. Zhang et al. [50] studied the phase transition in Ni-based HEAs under high pressures. For high-pressure experiments, the sample was loaded in the chamber, which was indented from the Re gasket with a pair of diamond anvils with a thickness of 40 μm . The single-phase CoCrFeNi HEA alloy was pressurized to observe the phase transition. A pressure-induced fcc-hcp phase transition was found in the CoCrFeNi HEA at the pressure of 13.5 GPa and at an ambient temperature. The hcp structure is recoverable when the pressure is released. The phase transformation is very sluggish and did not finish at 39 GPa

The HEA is essentially an alloy-design concept, and there is no requirement on which elements must be used. Therefore, it also provides a broad scope for the study of HEAs. The transition elements are the most frequently-used components of HEAs. As the major element in our planet, Fe is the most interesting element to be studied, and the phase transformations (including from bcc to hcp

structures) under high pressures or high temperature have already been found [51–53]. In ambient conditions, cobalt is in the hcp structure, and a pressure-induced phase transition to the fcc phase was found [54]. Figure 8 shows this pressure-induced phase transition. However, no pressure-induced phase transition was found in Ni up to 260 GPa [55]. [50].

Polymorphism is widely observed in many materials, which describes the occurrence of different lattice structures in a crystalline material, and is a potential research direction in the future. The polymorphism in the CoCrFeMnNi HEA is reported in [33]. By employing in situ, high-pressure, synchrotron radiation X-ray diffraction, the polymorphic transition from fcc to hcp structures in the CoCrFeMnNi HEA is observed. The hydrostatic pressure was up to 41 GPa using a DAC. The CoCrFeMnNi HEA has an fcc single-phase structure and remains stable up to 19.5 GPa. When the pressure reaches 22.1 GPa, new peaks appeared, indicating that the phase transition has occurred. All the new peaks revealed an fcc-to-hcp transition under high pressures. During the decompression, the phase transition was irreversible. Huang et al. [56] studied the deviatoric deformation kinetics in the CoCrFeMnNi HEA under hydrostatic compression. The HEA was subjected to a hydrostatic pressure of 20 GPa via a DAC. The main significance of this study was to provide another perspective for studying the deformation mode of the HEA system through high-pressure experiments [56].

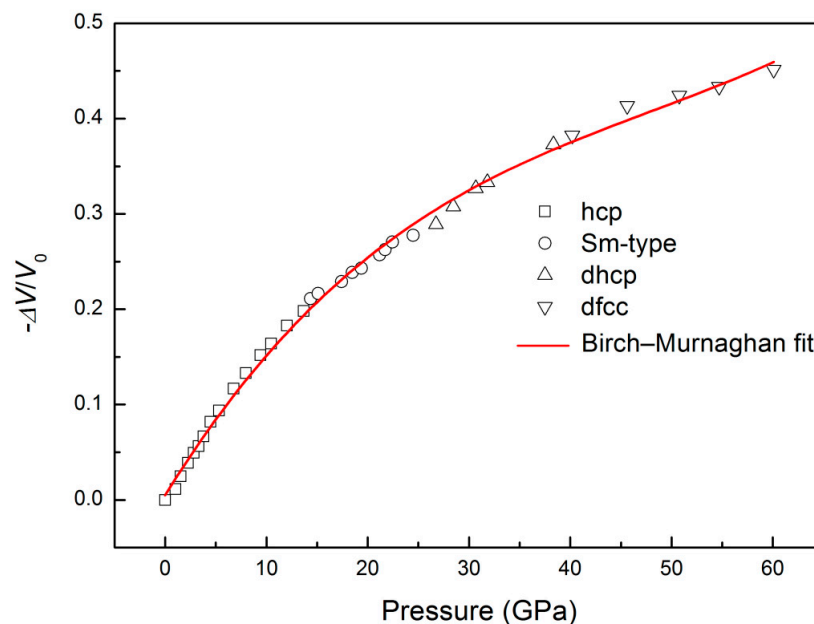


Figure 7. The measured pressure-volume relationship for various phases of the HoDyYGdTb high-entropy alloy (HEA) at up to 60.1 GPa, at room temperature, data from [47].

Gong Li et al. [57] studied the pressure-volume relationship of CoCrFeNiAlCu HEA using in-situ high-pressure energy-dispersive X-ray diffraction with synchrotron radiation at high pressures, and the results show that the CoCrFeNiAlCu HEA keeps a stable fcc + bcc structure in the experimental pressure ranges from 0 to 24 GPa. The equation of the state of the HEA determined by the calculation of the radial distribution function in the non-phase-transitional case is:

$$-\Delta V/V_0 = 2.7P - 0.256P^2 + 0.012P^3 - 2.928 \times 10^{-4}P^4 + 2.907 \times 10^{-6}P^5$$

where V_0 is the volume at zero pressure, $(\Delta V/V_0)$ is the relative volume change.

Cheng et al. [58] studied an ordered, bcc-structured (B2 phase) AlCoCrFeNi HEA using in situ, synchrotron radiation X-ray diffraction up to 42 GPa and non-in transmission electron microscopy. Pressure-induced polymorphic transitions (PIPT) to potentially disordered phase were observed. Yusenko et al. [59] studied the temperature and pressure stability for a hcp Ir_{0.19}Os_{0.22}Re_{0.21}Rh_{0.20}Ru_{0.19}

HEA. The sample was loaded in a DAC cell and did not result in phase transition with a maximum pressure of 45 GPa. Ahmad et al. [60] performed in-situ high-pressure and high-temperature XRD measurements on bcc-Hf₂₅Nb₂₅Zr₂₅Ti₂₅, fcc-Ni₂₀Co₂₀Fe₂₀Mn₂₀Cr₂₀ and hcp-Re₂₅Ru₂₅Co₂₅Fe₂₅ HEAs; all of the HEAs remained stable and no phase transition was observed.

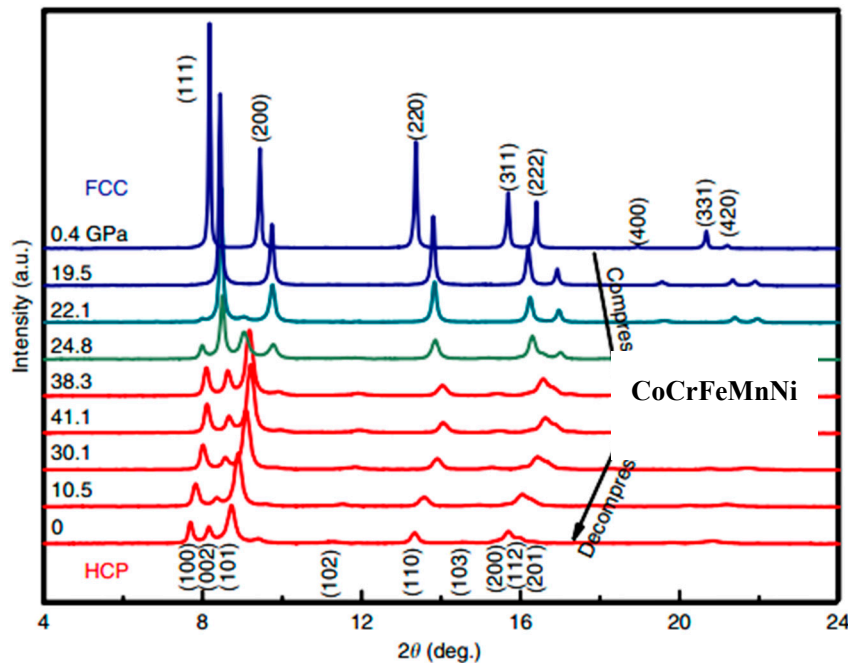


Figure 8. CoCrFeMnNi XRD patterns during compression and decompression, reproduced from [33], with permission from authors.

4.3. High-Pressure Torsion

Due to the severe lattice distortion effect and different chemical bonds of their constituent elements, the plastic deformation mechanisms of HEA could be different from that of conventional alloys. The high-pressure torsion (HPT) method is currently used mainly as a severe plastic deformation (SPD) technique for grain refinement, and it has taken a long time to synthesize a metastable phase by HPT processing. High-pressure torsion is generally used to prepare non-porous bulk ultrafine grain samples, which can generate large plastic deformation of the sample through shear stress ($\gamma = 10\text{--}100$) [61–64]. At present, there have been reports on high-entropy alloys treated by high pressure torsion. These reports are mainly focused on the face centered cubic HEAs. Tang [65] obtained the nano-scale Al_{0.3}CoCrFeNi HEA by HPT and studied the strengthening mechanism of the annealing process. Schuh [66] used high pressure torsion to treat the CoCrFeMnNi HEA; the grain can be refined to 50 nm, and the strength and hardness can be increased to 1950 MPa and 520 HV, respectively. After high-pressure torsion of the face centered cubic high-entropy alloy, the grain gradually refines as the strain increases. As shown in Figure 9, the plastic-deformation mechanism mainly includes dislocation slip and twinning.

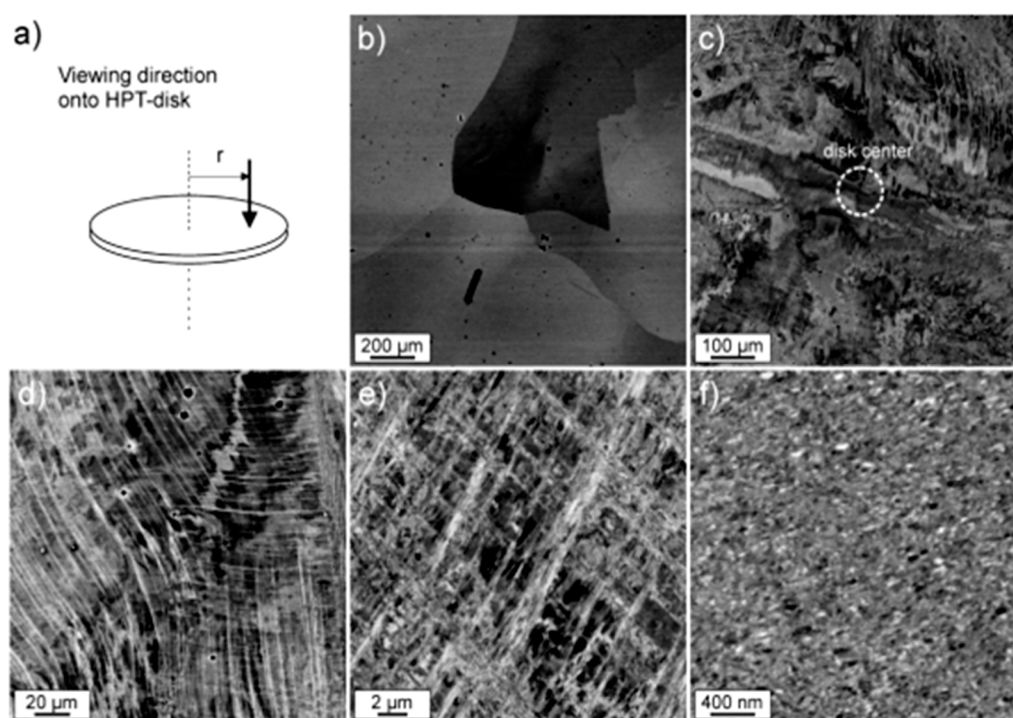


Figure 9. Microstructural evolution in HPT disks investigated with SEM using back-scattered electron contrast, reproduced from [66], with permission from authors.

Yu et al. showed that the plastic-deformation mechanisms of the single-phase fcc $\text{Al}_{0.1}\text{CoCrFeNi}$ HEA induced by HPT at room temperature [67]. The sample was prepared by arc-melting and then casted as a plate by vacuum induction. The plate was hot-isostatic pressed (HIPed) at 1473 K, and 100 MPa, for 4 h, and then placed in a horizontal tube furnace at 1423 K for 50 h. The samples were compressed at 6 GPa through 1 and 2 turns with the rotation speed of 1 rpm. Processing by HPT produces a very substantial grain refinement in HEAs. The deformation mechanisms include the dislocation slip and twinning at room temperature. As shown in Figure 10, the average Vickers microhardness of the HIPed sample is 135 Hv. After HPT for 1 revolution, the microhardness reaches a saturation of about 482 Hv at the edge of the sample.

A deformation-induced phase transformation in a single-phase fcc $\text{Co}_{20}\text{Cr}_{26}\text{Fe}_{20}\text{Mn}_{20}\text{Ni}_{14}$ HEA during the cryogenic HPT was reported [68]. The sample was prepared by arc-melting and then homogenizing by heat treatment at 1050 °C for 24 h; the sample was cold-rolled after the heat treatment, followed by annealing at 1050 °C for 1 h with water quenching. The HPT processing was performed at 77 K in the liquid nitrogen (cryo-HPT) and at room temperature (300 K-HPT), the samples were compressed at 5 GPa for 5 revolutions. The thermodynamic calculations indicated that the hcp phase showed a higher stability than the fcc phase. The cryo-HPT providing an extra driving force for the fcc to hcp phase transformation of the $\text{Co}_{20}\text{Cr}_{26}\text{Fe}_{20}\text{Mn}_{20}\text{Ni}_{14}$ alloy at 77 K. The XRD pattern of the annealed sample shows the FCC phase and the r phase. In contrast, there was no r phase in the XRD pattern of the 300 K-HPT or cryo-HPT treated samples. Only the fcc peak was found. The absence of the r-phase peak after HPT treatment may have been due to grain refinement and residual strain after HPT treatment, which causes the main fcc peak to broaden. Unlike other conditions, the XRD pattern of the low temperature and high pressure treated alloy contains a well-developed hcp peak. This gives us reason to assume that, unlike 300 K-HPT, low temperature HPT induces a phase transition of fcc-to-hcp [68]. Furthermore, the microstructure and thermal stability of the nanocrystalline CoCrFeMnNi HEA after HPT were reported, and the results indicated that the grain size was refined, along with an unusual increase of the strength [66]. The hardness of $\text{Al}_{0.3}\text{CoCrFeNi}$ was significantly increased processed by HPT [65].

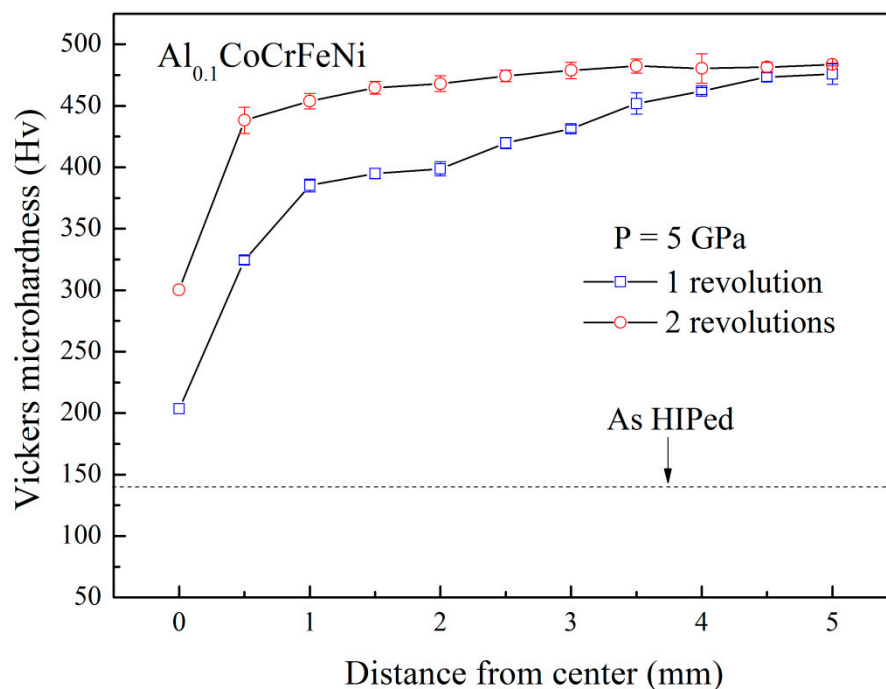


Figure 10. Vickers microhardness plotted against the distance from the center for the sample, data from [67].

4.4. Hexahedron Anvils Press

HEAs with high hardness prepared by high-pressure sintering were reported by Yu et al. [69]. The equiatomic CoCrFeNiCu and CoCrFeNiMn HEAs were prepared by high-pressure sintering (HPS). The elemental powders were developed in a planetary ball mill. Then the powders were sintered in the hexahedron anvil press at 1273 K and 5 GPa for 15 min. A graphite tube was taken as the heating device and the pyrophyllite as the pressure-transmitting medium. The structures and mechanical properties were carefully investigated. It revealed that the structure of the HEA powders have a main fcc phase and a minor bcc phase. After high-pressure sintering, the phase transition from the bcc to fcc structures occurred, and exhibited a simple solid-solution structure. The hardness of the CoCrFeNiCu HEA increased from 133 HV to 494 HV by HPS, and the hardness of the CoCrFeNiMn increased from 300 HV to 587 HV. The increase of hardness is the reason for the decrease of the grain size. The grain size is about 100 nm after HPS. It reveals that the HPS is an effective way to design excellent HEAs.

5. Future Work

HEAs are considered to be one of the three breakthroughs in alloying theory in recent decades (the other two are bulk metallic glass and metal rubber). There are huge developments underway for this unique design concept. The high mixing entropy makes it have an extensive application potential. Since the discovery of HEAs, it has been about two decades. Only in recent years, it has received sufficient attention from researchers and developed rapidly. There is still a great amount of work to be done. The high-pressure technology has been more and more widely used in the fields of fabricating the new material preparation and changing the structures and organizations of materials, such as synthesizing diamonds with the ultra-high-pressure technology, producing ultra-hard and antifricion materials, etc. The constant renewal of the high-pressure technology will enable the development of excellent and more promising materials. Additionally, high pressure science has obvious frontier characteristics, which brings forth many new opportunities and challenges for the development of science and technology. National security is a potentially important driving force of the international attention, in addition to mere intellectual interest and economic interests. HEAs will be an important

materials development route for the field of the high-pressure science in the future. The properties of HEAs change when high pressure act on the alloys. The most significant change in the alloys, due to the high pressure, is the phase change during the high-pressure crystallization. The materials show many unique properties under high pressures. The research of high entropy alloy under high pressure has already established a certain foundation, but the industrial applications have not matched the expected results. It is necessary to further broaden the application field, which will play a more important role in future theoretical improvement and new material preparation. With HEAs, as emerging alloys with a great potential for the future development, their structures and properties under high pressures need further studies.

6. Conclusions

HEAs as a new class of alloys have been attracting more and more attention in recent years. With the unique design concept, HEAs show wide application potentials. High pressure is an external condition that is important for structural changes and phase transitions. The unique phenomenon of HEAs under high pressures gives us a new understanding of HEAs, providing a new way forward for the in-depth study of HEAs. Some single-phase HEAs, such as CoCrFeNi, rare-earth HoDyYGdNb, and CoCrFeMnNi phase transition under high pressure, but bcc-Hf₂₅Nb₂₅Zr₂₅Ti₂₅, fcc-Ni₂₀Co₂₀Fe₂₀Mn₂₀Cr₂₀, and hcp-Re₂₅Ru₂₅Co₂₅Fe₂₅ remain stable and no phase transition is observed under high pressure. These unique structural changes and phase transitions of HEAs under high pressure show wide application potentials. As a new research trend, there is a growing interest in the structure and performance of HEAs under high pressures. The studies of HEAs under high pressures are summarized in this paper, with a hope to deepen the fundamental understanding of HEAs under high pressures.

Author Contributions: W.D. performed the data analyses and wrote the manuscript; Z.Z. helped perform the analysis with constructive discussions; M.Z. and Y.M. helped document retrieval; P.K.L. and P.Y. performed the manuscript review; G.L. contributed to the conception of the study.

Funding: This research received no external funding

Acknowledgments: One of the authors (Gong Li) acknowledges the National Science Foundation of China (Grant No. 11674274). Pengfei Yu acknowledges the National Natural Science Funds of China (Grant No. 51601166). Peter K. Liaw very much appreciates the support of the U.S. Army Research Office Projects (W911NF-13-1-0438 and W911NF-19-2-0049) with the program managers, M.P. Bakas, S. N. Mathaudhu, and D.M. Stepp. Peter K. Liaw thanks the support from the National Science Foundation (DMR-1611180 and 1809640) with the program directors, G. Shiflet and D. Farkas.

Conflicts of Interest: The authors declare no conflict of interest.

References

1. Wang, J.; Niu, S.Z.; Guo, T.; Kou, H.C.; Li, J.S. The FCC to BCC phase transformation kinetics in an Al_{0.5}CoCrFeNi high entropy alloy. *J. Alloy. Compd.* **2017**, *710*, 144–150. [[CrossRef](#)]
2. Otto, F.; Dlouhý, A.; Pradeep, K.G.; Kubenov, M.; Raabe, D.; Eggeler, G.; George, E.P. Decomposition of the single-phase high-entropy alloy CrMnFeCoNi after prolonged anneals at intermediate temperatures. *Acta Mater.* **2016**, *112*, 40–52. [[CrossRef](#)]
3. Stepanova, N.D.; Yurchenko, N.Y.; Panina, E.S.; Tikhonovsky, M.A.; Zharebtsov, S.V. Precipitation-strengthened refractory Al_{0.5}CrNbTi₂V_{0.5} high entropy alloy. *Mater. Lett.* **2017**, *188*, 162–164. [[CrossRef](#)]
4. Yeh, J.W.; Chen, S.K.; Lin, S.J. Nano structured high-entropy alloys with multiple principal elements: Novel alloy design concepts and outcomes. *Adv. Eng. Mater.* **2004**, *6*, 299–303. [[CrossRef](#)]
5. Cantor, B.; Chang, I.T.H.; Knight, P. Microstructural development in equiatomic multicomponent alloys. *Mater. Sci. Eng. A Struct. Mater. Prop. Microstruct. Process.* **2004**, *375*, 213–218. [[CrossRef](#)]
6. Deng, Y.; Asan, C.C.; Pradeepk, G. Design of a twinning-induced plasticity high entropy alloy. *Acta Mater.* **2015**, *94*, 124–133. [[CrossRef](#)]
7. Li, Z.; Pradeepk, G.; Deng, Y. Metastable high-entropy dual-phase alloys overcome the strength-ductility trade-off. *Nature* **2016**, *534*, 227–230. [[CrossRef](#)]

8. Senkov, O.N.; Wilks, G.B.; Miracle, D.B.; Chuang, C.P.; Liaw, P.K. Refractory high-entropy alloys. *Intermetallics* **2010**, *18*, 1758–1765. [[CrossRef](#)]
9. Yurchenko, N.Y.; Stepanov, N.D.; Shaysultanov, D.G. Effect of Al content on structure and mechanical properties of the $Al_xCrNbTiVZr$ ($x = 0; 0.25; 0.5; 1$) high-entropy alloys. *Mater. Charact.* **2016**, *121*, 125–134. [[CrossRef](#)]
10. Stepanov, N.D.; Yurchenko, N.Y.; Shaysultanov, D.G. Effect of Al on structure and mechanical properties of $Al_xNbTiVZr$ ($x = 0, 0.5, 1, 1.5$) high entropy alloys. *J. Mater. Sci. Technol.* **2015**, *31*, 1184–1193. [[CrossRef](#)]
11. Ashby, M.F. *Materials Selection in Mechanical Design*; Elsevier: Oxford, UK, 2011.
12. Yeh, J.W. Recent progress in high-entropy alloys. *Ann. Chim. Sci. Mater.* **2016**, *31*, 48–633. [[CrossRef](#)]
13. Zhang, Y.; Yang, X.; Liaw, P.K. Alloy design and properties optimization of high-entropy alloys. *J. Miner. Met. Mater. Soc.* **2012**, *64*, 830–838. [[CrossRef](#)]
14. Zhang, Y.; Zhou, Y.J.; Lin, J.P.; Chen, G.L.; Liaw, P.K. Solid-solution phase formation rules for multi-component alloys. *Adv. Eng. Mater.* **2008**, *10*, 534–538. [[CrossRef](#)]
15. Tsai, K.Y.; Tsai, M.H.; Yeh, J.W. Sluggish diffusion in Co-Cr-Fe-Mn-Ni high-entropy alloys. *Acta Mater.* **2013**, *61*, 4887–4897. [[CrossRef](#)]
16. Juan, C.C.; Hsu, C.Y.; Tsai, C.W. On microstructure and mechanical performance of $AlCoCrFeMo_{0.5}Ni_x$ high-entropy alloys. *Intermetallics* **2013**, *32*, 401–407. [[CrossRef](#)]
17. Ranganathan, S. Alloyed pleasures: Multimetallurgical cocktails. *Curr. Sci.* **2003**, *85*, 1404–1406.
18. Takeuchi, A.; Amiya, K.; Wada, T. High-entropy alloys with a hexagonal close-packed structure designed by equi-atomic alloy strategy and binary phase diagrams. *J. Miner. Met. Mater. Soc.* **2014**, *66*, 1984–1992. [[CrossRef](#)]
19. Chen, J.; Niu, P.; Liu, Y. Effect of Zr content on microstructure and mechanical properties of $AlCoCrFeNi$ high entropy alloy. *J. Mater. Des.* **2016**, *94*, 39–44. [[CrossRef](#)]
20. Hsu, C.Y.; Yeh, J.W.; Chen, S.K. Wear resistance and high-temperature compression strength of fcc $CuCoNiCrAl_{0.5}Fe$ alloy with boron addition. *Metall. Mater. Trans. A* **2004**, *35*, 1465–1469. [[CrossRef](#)]
21. Chen, M.; Lin, S.; Yeh, J.W. Effect of vanadium addition on the microstructure, hardness, and wear resistance of $Al_{0.5}CoCrCuFeNi$ high-entropy alloy. *Metall. Mater. Trans. A* **2006**, *37*, 1363–1369. [[CrossRef](#)]
22. Hsu, C.Y.; Sheu, T.S.; Yeh, J.W. Effect of iron content on wear behavior of $AlCoCrFeMo_{0.5}Ni$ high-entropy alloys. *Wear* **2010**, *268*, 653–659. [[CrossRef](#)]
23. Zhu, J.M.; Zhang, H.F.; Fu, H.M. Microstructures and compressive properties of multicomponent $AlCoCrCuFeNiMo_x$ alloys. *J. Alloy. Compd.* **2010**, *497*, 52–56. [[CrossRef](#)]
24. Takeuchi, A.; Chen, N.; Wada, T. $Pd_{20}Pt_{20}Cu_{20}Ni_{20}P_{20}$ high-entropy alloy as a bulk metallic glass in the centimeter. *Intermetallics* **2011**, *19*, 1546–1554. [[CrossRef](#)]
25. Gao, X.Q.; Zhao, K.; Ke, H.B. High mixing entropy bulk metallic glasses. *J. Non-Cryst. Solids* **2011**, *357*, 3557–3560. [[CrossRef](#)]
26. Ma, L.; Wang, L.; Zhang, T. Bulk glass formation of Ti-Zr-Hf-Cu-M (M=Fe, Co, Ni) alloys. *Mater. Trans.* **2002**, *43*, 277–280. [[CrossRef](#)]
27. Christian, J.W.; Mahajan, S. Deformation twinning. *Prog. Mater. Sci.* **1995**, *39*, 1–157. [[CrossRef](#)]
28. Jain, J.; Poole, W.J.; Sinclair, C.W.; Gharghoury, M.A. Reducing the tension-compression yield asymmetry in a Mg-8Al-0.5Zn alloy via precipitation. *Scr. Mater.* **2010**, *62*, 301–304. [[CrossRef](#)]
29. Wang, H.; Lee, S.Y.; Gharghoury, M.A.; Wu, P.D.; Yoon, S.G. Deformation behavior of Mg-8.5wt.%Al alloy under reverse loading investigated by in-situ neutron diffraction and elastic viscoplastic self-consistent modeling. *Acta Mater.* **2016**, *107*, 404–414. [[CrossRef](#)]
30. Murty, B.S.; Yeh, J.W.; Ranganathan, A.S. Chapter 2—High-entropy alloys: Basic concepts. *High. Entropy Alloy.* **2014**, 13–35.
31. Gludovatz, B.; Hohenwarter, A.; Catoor, D. A fracture-resistant high-entropy alloy for cryogenic applications. *Science* **2014**, *345*, 1153–1158. [[CrossRef](#)]
32. Chuang, M.H.; Tsai, M.H.; Wang, W.R. Microstructure and wear behavior of $Al_xCo_{1.5}CrFeNi_{1.5}Ti_y$ high-entropy alloys. *Acta Mater.* **2011**, *59*, 6308–6317. [[CrossRef](#)]
33. Zhang, F.; Wu, Y.; Lou, H.B.; Zeng, Z.D.; Prakapenka, V.B.; Greenberg, E.; Ren, Y.; Yan, J.Y.; Okasinski, J.S.; Liu, X.J.; et al. Polymorphism in a high-entropy alloy. *Nat. Commun.* **2017**, *8*, 15687. [[CrossRef](#)] [[PubMed](#)]
34. Miracle, D.B.; Senkov, O.N. A critical review of high entropy alloys and related concepts. *Acta Mater.* **2017**, *122*, 448–511. [[CrossRef](#)]

35. Zhang, Y.; Zuo, T.T.; Tang, Z.; Gao, M.C.; Dahmen, K.A.; Liaw, P.K.; Lu, Z.P. Microstructures and properties of high-entropy alloys. *Prog. Mater. Sci.* **2014**, *61*, 1–93. [[CrossRef](#)]
36. Porter, D.A.; Easterling, K.E.; Sherif, M.Y. *Phase Transformations in Metals Andalloys*; CRC Press: Boca Raton, FL, USA, 2009.
37. Hemley, R.J.; Ashcroft, N.W. The revealing role of pressure in the condensed matter sciences. *Phys. Today* **1998**, *8*, 26–27. [[CrossRef](#)]
38. Bundy, F.P.; Hall, H.T.; Strong, H. Man-made diamonds. *Nature* **1955**, *176*, 51–55. [[CrossRef](#)]
39. Chen, K.W.; Jian, S.R.; Wei, P.J. A study of the relationship between semi-circular shear bands and pop-ins induced by indentation in bulk metallic glasses. *Intermetallics* **2010**, *18*, 1572–1578. [[CrossRef](#)]
40. Faupel, F.; Rätzke, K.; Ehmler, H. Diffusion in metallic glasses and supercooled melts. *Rev. Mod. Phys.* **2000**, *644*, 237–280. [[CrossRef](#)]
41. Zhang, F.; Lou, H.B.; Cheng, B.Y.; Zeng, Z.D.; Zeng, Q.S. High-pressure induced phase transitions in high-entropy alloys: A review. *Entropy* **2019**, *21*, 239. [[CrossRef](#)]
42. Buras, B.; Olsen, J.S.; Gerward, L. X-ray energy-dispersive diffractometry using synchrotron radiation. *J. Appl. Crystallogr.* **1977**, *10*, 431–438. [[CrossRef](#)]
43. Dubrovinsky, L.; Dubrovinskaia, N.; Bykova, E. The most incompressible metal osmium at static pressures above 750 gigapascals. *Nature* **2015**, *525*, 226. [[CrossRef](#)] [[PubMed](#)]
44. Bridgman, P.W. Effects of high shearing stress combined with high hydrostatic pressure. *Phys. Rev.* **1935**, *48*, 825–847. [[CrossRef](#)]
45. Zhilyaev, A.P.; Langdon, T.G. Using high-pressure torsion for metal processing: Fundamentals and applications. *Prog. Mater. Sci.* **2008**, *53*, 893–979. [[CrossRef](#)]
46. Yao, Y.G.; Huang, Z.N.; Xie, P.F.; Lacey, S.D.; Jacob, R.J.; Xie, H.; Chen, F.; Nie, A.; Pu, T.; Rehwoldt, M. Carbothermal shock synthesis of high-entropy-alloy nanoparticles. *Science* **2018**, *359*, 1489–1494. [[CrossRef](#)] [[PubMed](#)]
47. Yu, P.F.; Zhang, L.J.; Ning, J.L. Pressure-induced phase transitions in HoDyYGd Tb high-entropy alloy. *Mater. Lett.* **2014**, *196*, 137–140. [[CrossRef](#)]
48. Francis, B. Finite strain isotherm and velocities for single-crystal and polycrystalline NaCl at high pressures and 300 K. *J. Geophys. Res. Solid Earth* **1978**, *83*, 1258–1263.
49. Dubrovinsky, L.; Dubrovinskaia, N.; Crichton, W.A.; Mikhaylushkin, A.S.; Simak, S.I.; Abrikosov, I.A.; Almeida, J.S.; Ahuja, R.; Luo, W.; Johansson, B. Noblest of all metals is structurally unstable at high pressure. *Phys. Rev. Lett.* **2007**, *98*, 045503. [[CrossRef](#)] [[PubMed](#)]
50. Zhang, F.X.; Zhao, S.J.; Jin, K.; Bei, H.; Popov, D.; Park, C.; Neuefeind, J.C.; Weber, W.J.; Zhang, Y.W. Pressure-induced fcc to hcp phase transition in Ni-based high entropy solid solution alloys. *Appl. Phys. Lett.* **2017**, *110*, 011902. [[CrossRef](#)]
51. Takahashi, T.; Bassett, W.A. High-pressure polymorph of iron. *Science* **1964**, *145*, 483–486. [[CrossRef](#)] [[PubMed](#)]
52. Saxena, S.K.; Shen, G.; Lazor, P. Experimental evidence for a new iron phase and implications for earth's core. *Science* **1993**, *260*, 1312–1314. [[CrossRef](#)] [[PubMed](#)]
53. Andrault, D.; Fiquet, G.; Kunz, M.; Visocekas, F.; Hausermann, D. The orthorhombic structure of iron: An in situ study at high-temperature and high-pressure. *Science* **1997**, *278*, 831–834. [[CrossRef](#)]
54. Yoo, C.S.; Cynn, H.; Soderlind, P.; Iota, V. New beta (fcc)—Cobalt to 210 GPa. *Phys. Rev. Lett.* **2000**, *84*, 4132. [[CrossRef](#)] [[PubMed](#)]
55. Sergueev, I.; Dubrovinsky, L.; Ekholm, M.; Yekilova, O.Y.; Chumakov, A.I.; Zajac, M.; Potapkin, V.; Kantor, I.; Bornemann, S.; Ebert, H.; et al. Hyperfine splitting and room-temperature ferromagnetism of Ni at multimegabar pressure. *Phys. Rev. Lett.* **2013**, *111*, 157–601. [[CrossRef](#)] [[PubMed](#)]
56. Huang, E.W.; Lin, C.M.; Juang, J.Y.; Chang, Y.J.; Chang, Y.W.; Wu, C.S.; Tsai, C.W.; Yeh, A.C.; Shieh, S.R. Deviatoric deformation kinetics in high entropy alloy under hydrostatic compression. *J. Alloy. Compd.* **2019**, *349*, 50113. [[CrossRef](#)]
57. Li, G.; Xiao, D.H.; Yu, P.F.; Zhang, L.J.; Liaw, P.K.; Li, Y.C.; Liu, R.P. Equation of state of an AlCoCrCuFeNi high-entropy alloy. *JOM* **2015**, *67*, 2310–2313. [[CrossRef](#)]
58. Cheng, B.Y.; Zhang, F.; Lou, H.b.; Chen, X.H.; Liaw, P.K.; Yan, J.Y.; Zeng, Z.D.; Ding, Y.; Zeng, Q.S. Pressure-induced phase transition in the AlCoCrFeNi high-entropy alloy. *Scr. Mater.* **2019**, *161*, 82–92. [[CrossRef](#)]

59. Yusenkov, K.V.; Riva, S.; Carvalho, P.A.; Yusenkov, M.V.; Arnaboldi, S.; Sukhikh, A.S.; Hanfland, M.; Gromilov, S.A. First hexagonal close packed high-entropy alloy with outstanding stability under extreme conditions and electrocatalytic activity for methanol oxidation. *Scr. Mater.* **2017**, *138*, 22–27. [[CrossRef](#)]
60. Ahmad, A.S.; Su, Y.; Liu, S.Y.; Ståhl, K.; Wu, Y.D.; Hui, X.D.; Ruett, U.; Gutowski, O.; Glazyrin, K.; Liermann, H.P.; et al. Structural stability of high entropy alloys under pressure and temperature. *J. Appl. Phys.* **2017**, *121*, 235901. [[CrossRef](#)]
61. Valiev, R.Z.; Estrin, Y.; Horita, Z. Producing bulk ultrafine-grained materials by severe plastic deformation. *J. Miner. Met. Mater. Soc.* **2010**, *58*, 33–39. [[CrossRef](#)]
62. Zhilyaev, A.P.; Lee, S.; Nurislamova, G.V. Microhardness and microstructural evolution in pure nickel during high-pressure torsion. *Scr. Mater.* **2001**, *44*, 2753–2758. [[CrossRef](#)]
63. Révész, A.; Hóbor, S.; Lábár, J.L. Partial amorphization of a Cu–Zr–Ti alloy by high pressure torsion. *J. Appl. Phys.* **2006**, *100*, 103522. [[CrossRef](#)]
64. Sabirov, I.; Pippan, R. Formation of a W-25%Cu nanocomposite during high pressure torsion. *Scr. Mater.* **2005**, *52*, 1293–1298. [[CrossRef](#)]
65. Tang, Q.H.; Huang, Y.; Huang, Y.Y. Hardening of an Al_{0.3}CoCrFeNi high entropy alloy via high-pressure torsion and thermal annealing. *Mater. Lett.* **2015**, *151*, 126–129. [[CrossRef](#)]
66. Schuh, B.; Mendez-Martin, F.; Völker, B.; George, E.P.; Clemens, H.; Pippan, R.; Hohenwarter, A. Mechanical properties, microstructure and thermal stability of a nanocrystalline CoCrFeMnNi high-entropy alloy after severe plastic deformation. *Acta Mater.* **2015**, *96*, 258–268. [[CrossRef](#)]
67. Yu, P.F.; Cheng, H.; Zhang, L.J.; Zhang, H. Effects of high pressure torsion on microstructures and properties of an Al_{0.1}CoCrFeNi high-entropy alloy. *Mater. Sci. Eng.* **2016**, *655*, 283–291. [[CrossRef](#)]
68. Moon, J.; Qi, Y.; Tabachnikova, E.; Estrin, Y.; Choi, W.M. Deformation-induced phase transformation of Co₂₀Cr₂₆Fe₂₀Mn₂₀Ni₁₄ high-entropy alloy during high-pressure torsion at 77 K. *Mater. Lett.* **2017**, *202*, 86–88. [[CrossRef](#)]
69. Yu, P.F.; Zhang, L.J.; Cheng, H.; Zhang, H.; Ma, M.Z.; Li, Y.C.; Li, G.; Liaw, P.K.; Liu, R.P. The high-entropy alloys with high hardness and soft magnetic property prepared by mechanical alloying and high-pressure sintering. *Intermetallics* **2016**, *70*, 82–87. [[CrossRef](#)]



© 2019 by the authors. Licensee MDPI, Basel, Switzerland. This article is an open access article distributed under the terms and conditions of the Creative Commons Attribution (CC BY) license (<http://creativecommons.org/licenses/by/4.0/>).